

15386
KREEP Basalt
7.5 grams

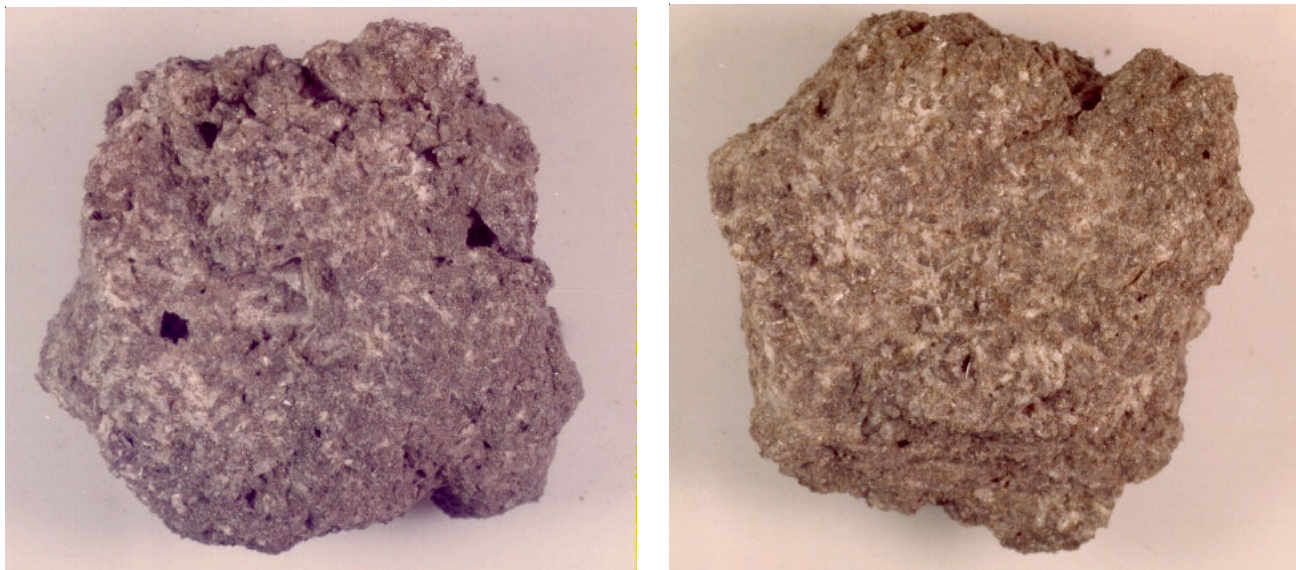


Figure 1: Photos of front and back of 15386. Rock is 2 cm across. NASA #s S76-24073 and 24072.

Introduction

15386 is the largest sample of pristine KREEP basalt in the collection (figure 1). By pristine we mean that it is lacking in meteoritical siderophiles (Ir, Re, Au etc), and hence not contaminated by meteorite debris. Thus it is thought to represent an indigenous lunar volcanic melt derived from the lunar interior (see discussion in 15382).

Petrography

Steele et al. (1972) and Takeda et al. (1978) give very brief descriptions of 15386. Plagioclase laths are surrounded by interstitial pyroxene (figure 2). The mesostasis has significant cristobalite (10%), ilmenite plates (3%), and minor phosphate, iron and sulfide.

Mineralogy

Pyroxene: The cores of pyroxene crystals are Mg-rich orthopyroxene (Takeda et al. 1978). They are surrounded (overgrown) by pigeonite with patches or rims of subcalcic augite (figure 3).

Plagioclase: Steele et al. (1972) report that plagioclase in 15386 is An_{85-70} and contains minor amounts of FeO (0.2 wt %).

Cristobalite: Steele et al. (1972) report a significant amount of cristobalite (10%).

Opaques: Not studied.

Mineralogical Mode for 15386

	Steele et al. 1972	Simonds et al. 1975	Taylor et al. 1991
Pyroxene	50 %	50	43
Plagioclase	35		43
Cristobalite	10		8
Ilmenite	3		3
mesostasis			

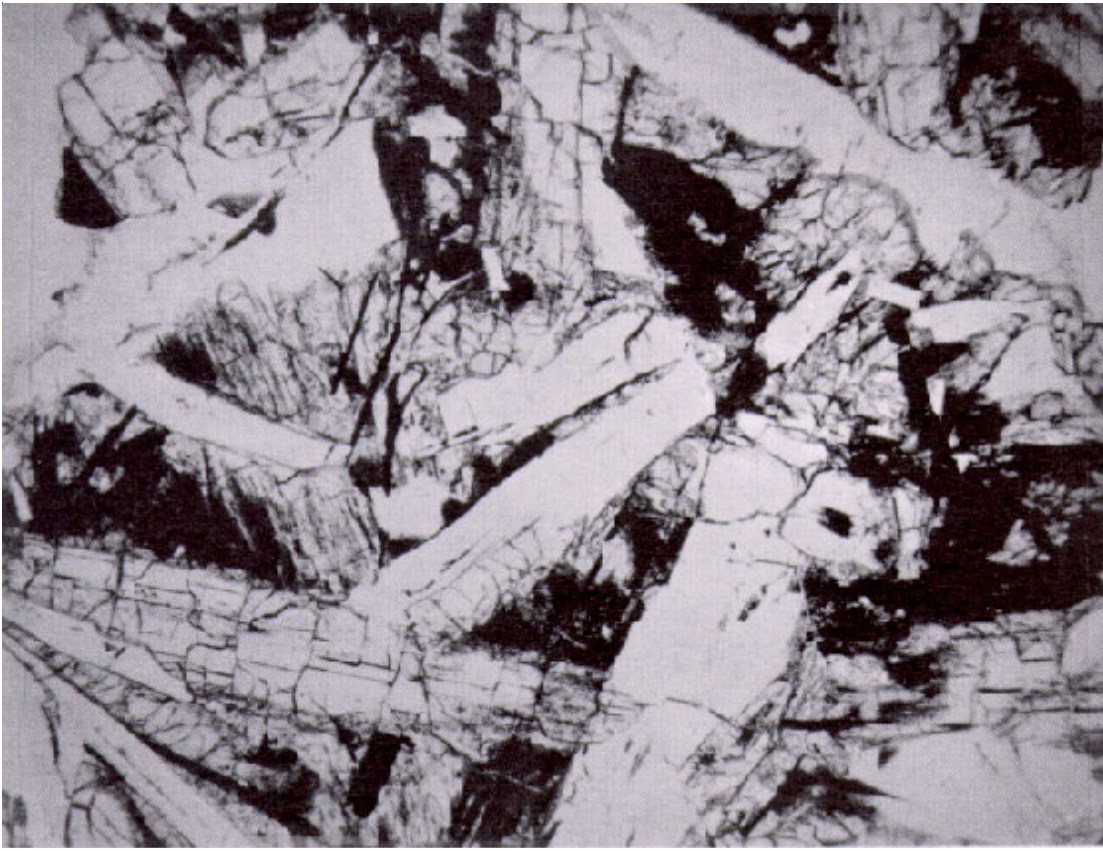


Figure 2: Photomicrograph of thin section of 15386. Field of view 2 mm.

Mesostasis: The mesostasis in 15386 was studied by Takeda et al. (1984) who found that the REE were located in whitlockite.

Chemistry

The chemical composition of 15386 is tabulated in table 1. The rare-earth-element pattern is parallel to that of “KREEP” (figure 4). When the major element composition is plotted on the Si-Ol-An pseudoternary phase diagram (figure 7), 15386 is found to be on the liquidus between plagioclase and pyroxene. Meteoritical siderophiles are low and, thus, this sample of KREEP is judged to be pristine (Ebihara et al. 1992, Warren and Wasson 1978).

Radiogenic age dating

Nyquist et al. (1975) and Carlson and Lugmair (1979) determined the age of 15386 by Rb/Sr and Sm/Nd internal mineral isochrons (figures 5 and 6).

Carlson and Lugmair (1979) determined the whole rock Sm and Nd isotopic composition and calculated the “whole rock” age at ~ 4.36 b.y. which is interpreted by

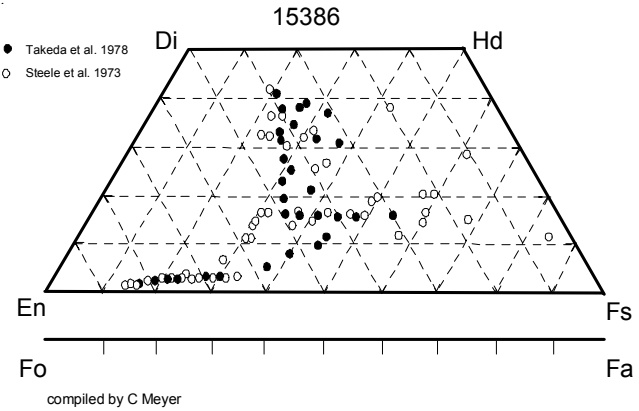


Figure 3: Pyroxene diagram for 15386 with data replotted from Steele et al. (1972) and Takeda et al. (1978). There is no olivine.

them as the closure age of the initial global scale lunar differentiation.

Unruh and Tatsumoto (1983) reported Lu and Hf isotopes and Lee et al. (1997) determined the W isotopes in 15386.

The age of Apollo 15 KREEP basalts (~ 3.9 b.y.) is indistinguishable from the age of the Imbrium basin.

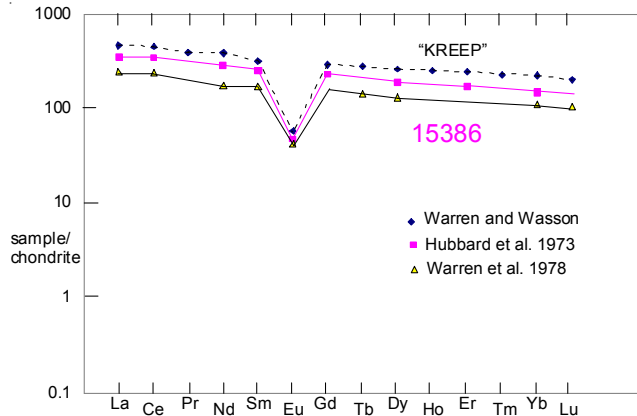


Figure 4: Normalized rare-earth-element diagram for 15386 with data from Hubbard et al. (1973) and Warren et al. (1978). Data for "KREEP" is included for comparison.

Cosmogenic isotopes and exposure ages

O'Kelley et al. (1976) determined ^{26}Al as $94 \pm 9 \text{ dpm/kg}$.

Other Studies

Walker et al. (1973) first determined the phase diagram for nonmare lunar basalts (figure 7). The composition of 15386 lies near the cotectic between plagioclase and pyroxene.

Crystallization experiments on KREEP-like liquids have been reported by Irving (1977), Rutherford et al. (1980), and Dickinson and Hess (1982).

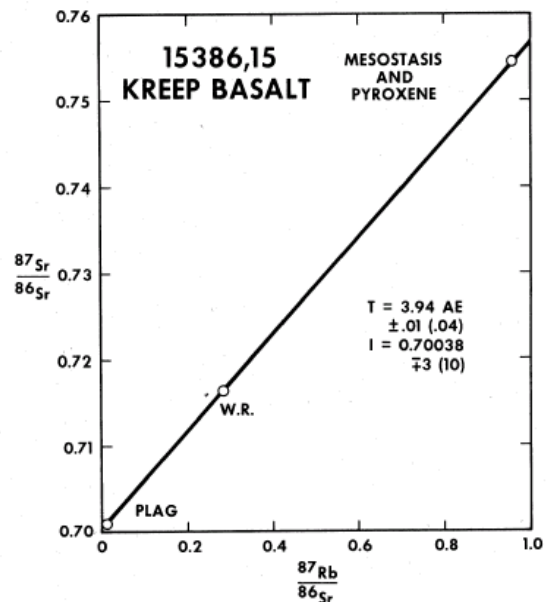


Figure 5: Rb-Sr internal mineral isochron for 15386 from Nyquist et al. (1975).

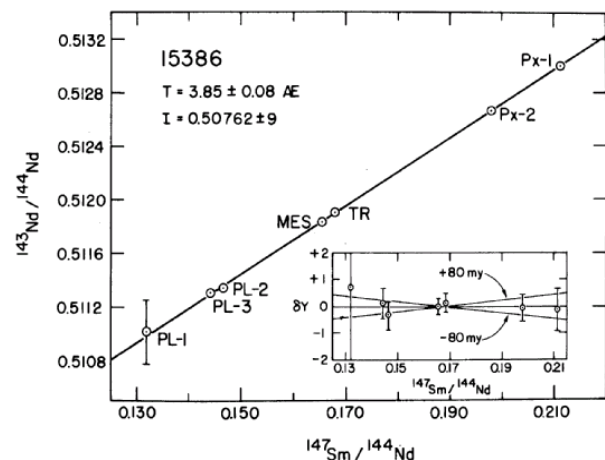


Figure 6: Sm-Nd internal mineral isochron for 15386 from Carlson and Lugmair (1979).

Summary of Age Data for 15386

	Rb/Sr	Ar/Ar	Sm/Nd
Nyquist et al. 1975	3.94 ± 0.01		
Carlson and Lugmair 1979			3.85 ± 0.08
Caution: These ages have not been corrected for new decay constants.			

Table 1. Chemical composition of 15386.

	O'Kelley	76	Hubbard	74	Rhodes	73	Warren	78	Ebihara	92	Nyquist	75	Carlson	79	Unruh	84	Lee	97	
reference																			
weight																			
SiO ₂ %						50.83	(c)												
TiO ₂		2.25	(b)	2.23	(c)	1.93	(d)												
Al ₂ O ₃				14.77	(c)	15.3	(d)												
FeO				10.55	(c)	10.16	(d)												
MnO				0.16	(c)	0.148	(d)												
MgO				8.17	(c)	10.44	(d)												
CaO				9.71	(c)	9.51	(d)												
Na ₂ O		0.82	(b)	0.73	(c)	0.82	(d)												
K ₂ O	0.6	(a)	0.69	(b)	0.67	(c)	0.5	(d)											
P ₂ O ₅				0.7	(c)														
S %				0.09	(c)														
sum				98.61															
Sc ppm					22	(d)													
V					62	(d)													
Cr					2430	(d)													
Co					23	(d)													
Ni					12.5	(d)	6.42	(e)											
Cu																			
Zn					3.5	(d)	2.56	(e)											
Ga					6.2	(d)													
Ge ppb					61	(d)	65.6	(e)											
As																			
Se						67.6	(e)												
Rb	18.46	(b)			14	(d)	17	(e)	18.46								(b)		
Sr	187	(b)							187.4								(b)		
Y																			
Zr					970	(d)													
Nb																			
Mo																			
Ru																			
Rh																			
Pd ppb						<0.8	(e)												
Ag ppb						0.592	(e)												
Cd ppb					10	(d)	8.56	(e)											
In ppb					1.8	(d)	2.38	(e)											
Sn ppb							0.605	(e)											
Sb ppb							<1.8	(e)											
Te ppb																			
Cs ppm					0.8	(d)	0.746	(e)											
Ba	837	(b)			650	(d)													
La	83.5	(b)			58	(d)													
Ce	211	(b)			147	(d)													
Pr																			
Nd	131	(b)			80	(d)					129.6						(b)		
Sm	37.5	(b)			25.5	(d)					36						(b)		
Eu	2.72	(b)			2.4	(d)													
Gd	45.4	(b)																	
Tb					5.3	(d)													
Dy	46.3	(b)			32	(d)													
Ho																			
Er	27.3	(b)																	
Tm																			
Yb	24.4	(b)			18.2	(d)													
Lu					2.58	(d)					3.193								
Hf					21	(d)					26.228								
Ta					2.4	(d)					30.51								
W ppb												1743							
Re ppb							0.016	(e)											
Os ppb							<0.09	(e)											
Ir ppb							0.061	(d)	0.004	(e)									
Pt ppb																			
Au ppb						0.22	(d)	0.012	(e)										
Th ppm	11.8	(a)	13.7	(b)		10	(d)												
U ppm	3.3	(a)	3.98	(b)		2.8	(d)	3.75	(e)										
technique	(a)	radiation counting,	(b)	IDMS,	(c)	XRF,	(d)	INAA,	RNAA,	(e)	RNAA								

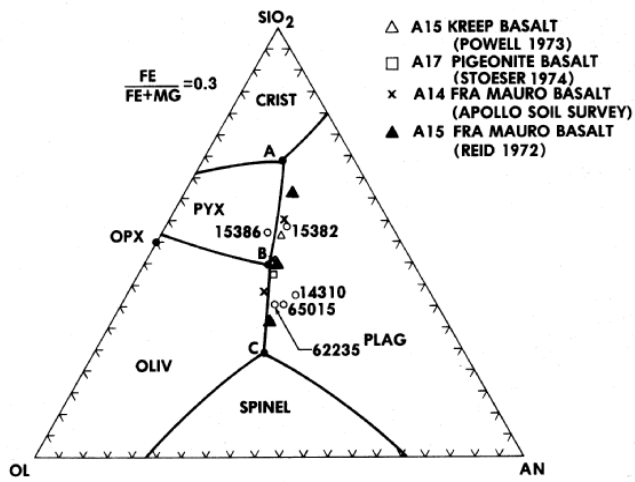


Figure 7: Projection of phase diagram for Fe/Fe+Mg = 0.3 as determined by Walker et al. (1973), showing that the composition of 15386 is near the cotectic between pyroxene and plagioclase (figure from Meyer 1977).

